

See discussions, stats, and author profiles for this publication at: <https://www.researchgate.net/publication/231444468>

# Stable simple enols. 23. Solid-state structures of 1-alkyl-2,2-dimesitylethenols. Application of the principle of structural correlation to ring-flip processes in 1,1-diarylvinyl s...

ARTICLE *in* JOURNAL OF THE AMERICAN CHEMICAL SOCIETY · OCTOBER 1989

Impact Factor: 12.11 · DOI: 10.1021/ja00203a019

---

CITATIONS

42

---

READS

5

## 4 AUTHORS, INCLUDING:



Menahem Kaftory

Technion - Israel Institute of Technology

178 PUBLICATIONS 1,525 CITATIONS

SEE PROFILE



David Nugiel

Camden County College

41 PUBLICATIONS 1,044 CITATIONS

SEE PROFILE

## At the completion of the reaction

$$[RT_{\infty}] + [ROH_{\infty}] = [RX_0] \quad (A7)$$

$$[RT_{\infty}] + [T_{\infty}] = [T_0] \quad (A8)$$

At intermediate time  $t$ 

$$[RT] + [ROH] + [RX] = [RX_0] \quad (A9)$$

$$[RT] + [T] = [T_0] \quad (A10)$$

and therefore

$$[T_0] - [T] + [ROH] + [RX] = [RX_0] \quad (A11)$$

## For the rate equations

$$-d[T]/dt = k_T[T][RX] \quad (A12)$$

$$d[ROH]/dt = k_w[RX] \quad (A13)$$

Divide eq A12 by eq A13

$$-d[T]/d[ROH] = k_T[T]/k_w = t[T] \quad (A14)$$

where  $t = k_T/k_w$  = trapping ratio. From eq A11

$$d[ROH] = d[T] - d[RX] \quad (A15)$$

Substituting into eq A14 and rearranging yield

$$d[T]/[T] = td[RX] - td[T] \quad (A16)$$

Integration gives

$$\ln [T] = t([RX] - [T]) + C \quad (A17)$$

At start of reaction,  $[T] = [T_0]$  and  $[RX] = [RX_0]$  (eq A1 and A3), therefore

$$C = \ln [T_0] - t([RX_0] - [T_0]) \quad (A18)$$

$$\ln [T]/[T_0] = t([RX] - [T]) - t([RX_0] - [T_0]) \quad (A19)$$

Measurement of thiol is made at completion of reaction, where  $[T] = [T_{\infty}]$  and  $[RX] = [RX_{\infty}]$ :

$$\ln [T_{\infty}]/[T_0] = t([T_0] - [T_{\infty}] - [RX_0]) \quad (A20)$$

Rearranging gives

$$t = (\ln [T_{\infty}]/[T_0]) / ([T_0](1 - [T_{\infty}]/[T_0] - [RX_0]/[T_0])) \quad (A21)$$

## Define

$$A_0 = \text{absorbance produced by thiol no substrate} = \epsilon[T_0] \quad (A22)$$

$$A = \text{absorbance produced by thiol remaining after reaction} = \epsilon[T_{\infty}] \quad (A23)$$

Therefore

$$t = (\ln A/A_0) / ([T_0](1 - A/A_0 - [RX_0]/[T_0])) \quad (A24)$$

## Solid-State Structures of 1-Alkyl-2,2-dimesitylethenols. Application of the Principle of Structural Correlation to Ring-Flip Processes in 1,1-Diarylvinyll Systems<sup>1</sup>

Menahem Kaftory,<sup>\*,†</sup> David A. Nugiel,<sup>‡</sup> Silvio E. Biali,<sup>\*,‡</sup> and Zvi Rappoport<sup>\*,‡</sup>

Contribution from the Department of Chemistry, Technion-Israel Institute of Technology, Haifa 32000, Israel, and Department of Organic Chemistry, The Hebrew University of Jerusalem, Jerusalem 91904, Israel. Received March 27, 1989

**Abstract:** The solid-state structures of 1-R-2,2-dimesitylethenols (R = H, Me, Et, *i*-Pr, *t*-Bu (**1a-e**)) and of 1,1-dimesitylethylene (**4**) were determined by X-ray diffraction. Enol **1a** displayed tetramers of four crystallographically independent molecules in the unit cell, and **1b** crystallized with an EtOH molecule. As the bulk of R is increased, the C=C bond length increases, the R-C=C bond angle ( $\alpha_4$ ) opens from 118.1° (**1a**) to 133.2° (**1e**), the RCO bond angle closes from 118.7° (**1a**) to 107.4° (**1e**), and the torsional angles  $\phi_1$  (of the Ar group cis to the OH) and  $\phi_2$  (of the aryl group trans to the OH) increase.  $\alpha_4$  is linear in Taft's  $E_s$  steric parameter. These trends are reproduced by MM2(85) calculations. Intermolecular enol-enol and enol-EtOH and intramolecular  $\pi$  (Ar)-HO hydrogen bonding are observed. The potential energy surface for 1,1-diphenylethylene (**8**) was calculated by molecular mechanics, and a propeller conformation with  $\phi_1 = \phi_2 = 40^\circ$  is the lowest energy conformer. The calculated enantiomerization barriers for correlated rotations of zero-, one-, and two-ring flips are 12.9, 1.2, and 3.0 kcal mol<sup>-1</sup>. In the calculated transition state for the zero-ring flip, both rings are puckered. The Cambridge Structural Database gave 116 crystallographically independent molecules with the Ar<sub>2</sub>C=CR<sup>1</sup>R<sup>2</sup> subunit. The  $\phi_1$  vs  $\phi_2$  angles for the 1,1-diarylethenes were superimposed on the calculated surface for **8** in a conformational map. Experimental points concentrate around the calculated minimum and are absent in the vicinity of the (0°, 0°) region. When R<sup>1</sup> and R<sup>2</sup> differ much in bulk, the points prefer to concentrate around (0°, 90°) and (90°, 0°) diagonal whereas when the bulk of R<sup>1</sup> resembles that of R<sup>2</sup>, many points concentrate along the diagonal between (40°, 40°) and (90°, 90°). By the crystal structure correlation principle, the one- and the two-ring flips are clearly favored over the zero-ring flip. Trimesityl-substituted systems are displaced toward the (90°, 90°) region compared with other triarylvinyll systems. Correlations between the bond angle ArCAr and the sum  $\phi_1 + \phi_2$  and between the C-Ar bond length and the bond angle ArC=C were found.

Recent investigations on the structures, the  $K_{\text{enol}}$  values (= [enol/ketone] at equilibrium), and dynamic behavior of stable simple enols—the crowded tri- and diarylethenols—showed the importance of steric effects on several phenomena.<sup>2</sup> (a) The  $\Delta G^\circ$  values for the ketone  $\rightleftharpoons$  enol equilibria for 1-alkyl-substituted and unsubstituted 2,2-dimesityl ethenols **1a-e** decrease linearly with

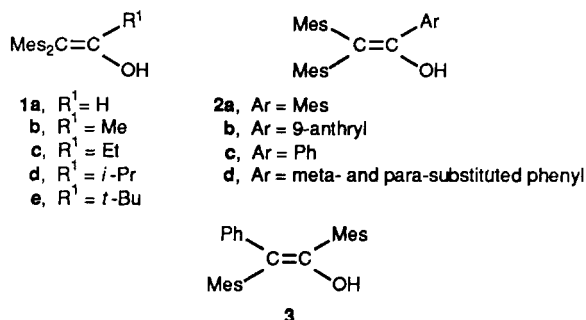
Taft's  $E_s$  values.<sup>3</sup> (b) The  $K_{\text{enol}}$  values for 1-aryl-2,2-dimesitylethenols **2** increase with the increased steric bulk of the aryl

(1) (a) Stable Simple Enols. 23. Part 22: Rappoport, Z.; Biali, S. E. *Acc. Chem. Res.* **1988**, *21*, 452. (b) Part 21: Nadler, E. B.; Rappoport, Z. *J. Am. Chem. Soc.* **1989**, *111*, 213.

(2) For a review on simple or stable enols see: (a) Capon, B.; Guo, B.-Z.; Kwok, F. C.; Siddhanta, A. K.; Zucco, C. *Acc. Chem. Res.* **1988**, *21*, 135. (b) Hart, H. *Chem. Rev.* **1979**, *79*, 515. (c) Reference 1a.

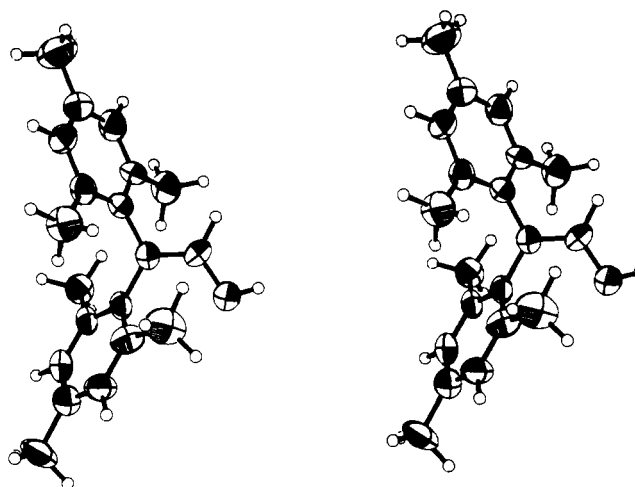
<sup>†</sup> Technion-Israel Institute of Technology.

<sup>‡</sup> The Hebrew University of Jerusalem.

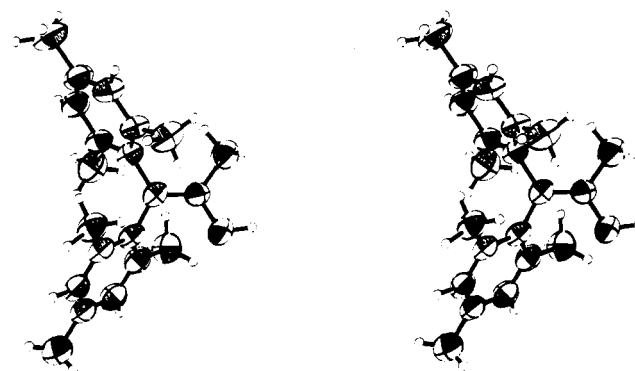


group.<sup>4</sup> (c) The rotational mechanism of lowest activation energy leading to enantiomerization in **1a-e**<sup>5a,b</sup> and in triarylethenols **2a,b** and related species depends on the bulk of R or Ar.<sup>5c,d</sup> The rotational barriers ( $\Delta G_c^\ddagger$ ) for **1a-e** are linear with  $E_s$  values.<sup>5b</sup> (d) The association constants for the enols with a single bulky group in binary  $\text{CCl}_4$ -DMSO mixtures show small sensitivity to steric effects.<sup>6</sup> (e) The ion radicals of **1**, **2a**, and **2d** display in the gas phase an unusual reciprocal Me/H transfer.<sup>7</sup> (f) Isotopomeric 1,2-dimesityl-2-(mesityl-*methyl-d*<sub>9</sub>)ethenols show an equilibrium steric isotope effect.<sup>8</sup> (g) Solid-state structures of enols **2a**, **2b**-EtOH, and **3** show the effect of the steric bulk on the torsional angles of the aryl groups and the bond angles.<sup>9</sup>

Determination of the solid-state structures of many crowded enols is therefore highly important for a better understanding of the above-mentioned phenomena in solution and in the gas phase. Inspection of the Cambridge Structural Database (1987 release)<sup>10</sup> revealed a large number of enol structures, but most of them are not "simple" (i.e., substituted only by H, R, and Ar) and involve internally strong hydrogen bonds. A recent paper<sup>11</sup> analyzed the data for the enol form derived from  $\beta$ -diketones by crystal structure correlations.<sup>12</sup> However, although our previous determination of the solid-state structures of some triarylethenols<sup>9</sup> supplied important information on their crowding, on the conformation of the OH, and on the torsional and bond angles, the number of structures studied was limited. Due to the varied nature of the enols, it was difficult to find a systematic correlation between the solid-state structure and the properties of the enols in solution. The availability of the series of crystalline enols **1a-e**, where the bulk at C(1) increases regularly and where the parameter representing this bulk ( $E_s$ ) is linearly correlated both with the static  $\Delta G^\circ$  property,<sup>3</sup> and the dynamic  $\Delta G_c^\ddagger$ ,<sup>5b</sup> presents a unique opportunity for a more regular search for correlations between the solid-state structure and the solution behavior of a family of enols.



**Figure 1.** Stereoscopic view of one of the four independent crystallographic molecules of **1a**.

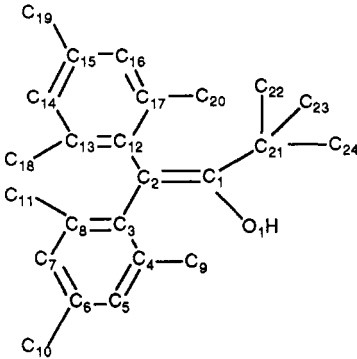


**Figure 2.** Stereoscopic view of **1b**. The associated EtOH molecule was omitted for clarity.

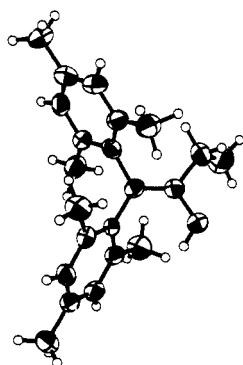
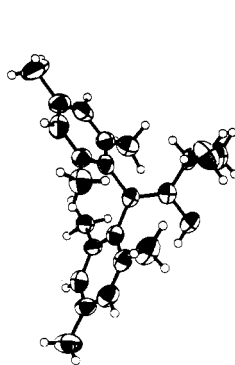
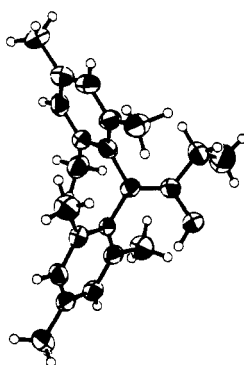
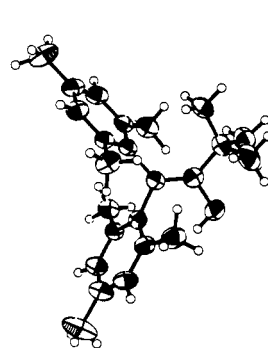
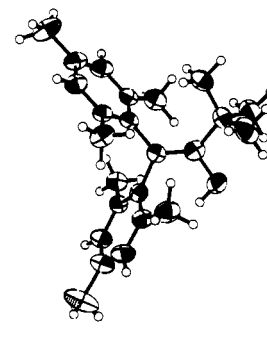
We therefore determined the crystal structure of enols **1a-e** with six goals, listed in the order of increased generality: (a) To extend our knowledge on the conformation of the enolic OH group in the solid state, as related to inter- and intramolecular hydrogen bonding and to compare it with that in solution. (b) To ascertain the preferred conformation of the alkyl substituent in **1b-e**, especially in relation to the direction of a C-H bond instead of a C-C bond to the site of higher steric crowding. Particularly interesting is the dihedral  $\text{C}=\text{C}-\text{C}-\text{H}$  angle in **1d**, which was estimated from the coupling constant  $^4J_{\text{HOCCH}}$  between the enolic and the isopropyl methine protons to be close to  $0^\circ$ .<sup>6b</sup> (c) To gather structural data (bond lengths and angles) on simple enols, since only a limited number of crystal structures of simple enols are available.<sup>9,13</sup> (d) To search for systematic changes in bond angles, torsional angles, and bond lengths accompanying the change in the bulk of R<sup>1</sup>. Especially interesting will be a correlation of these structural data with  $E_s$  values, which will connect structure, equilibria, and dynamic behavior.<sup>5b</sup> (e) Since triarylethenyl systems, including the ethenols, exist in the solid state in a propeller conformation in which all the rings are twisted in the same direction,<sup>9,14</sup> and a propeller is also the low-energy conformation of **1a-e** according to molecular mechanics calculations (MM2(85) program),<sup>5b</sup> it is of interest to find out whether this arrangement will be observed in the solid state. (f) To find out whether the propeller conformation indeed represents the preferred arrange-

- (3) Nugiel, D. A.; Rappoport, Z. *J. Am. Chem. Soc.* **1985**, *107*, 3669.  
 (4) (a) Biali, S. E.; Rappoport, Z. *J. Am. Chem. Soc.* **1985**, *107*, 1007. (b) Nadler, E. B.; Rappoport, Z. *Ibid.* **1987**, *109*, 2112.  
 (5) (a) Nugiel, D. A.; Biali, S. E.; Rappoport, Z. *J. Am. Chem. Soc.* **1984**, *106*, 3357. (b) Biali, S. E.; Nugiel, D. A.; Rappoport, Z. *Ibid.* **1989**, *111*, 846.  
 (6) (a) Biali, S. E.; Rappoport, Z. *Ibid.* **1984**, *106*, 477. (d) Biali, S. E.; Rappoport, Z. *J. Org. Chem.* **1986**, *51*, 2245.  
 (7) (a) Biali, S. E.; Rappoport, Z. *J. Am. Chem. Soc.* **1984**, *106*, 5641. (b) Rappoport, Z.; Nugiel, D. A.; Biali, S. E. *J. Org. Chem.* **1988**, *53*, 4814.  
 (8) (a) Biali, S. E.; Depke, G.; Rappoport, Z.; Schwarz, H. *J. Am. Chem. Soc.* **1984**, *106*, 496. (b) Rabin, I.; Biali, S. E.; Rappoport, Z.; Lifshitz, C. *Int. J. Mass. Spectrom. Ion Processes* **1986**, *70*, 301. (c) Uggerud, E.; Drewello, T.; Schwarz, H.; Nadler, E. B.; Biali, S. E.; Rappoport, Z. *Ibid.* **1986**, *71*, 287.  
 (9) Biali, S. E.; Rappoport, Z.; Hull, W. E. *J. Am. Chem. Soc.* **1985**, *107*, 5450.  
 (10) Kaftory, M.; Biali, S. E.; Rappoport, Z. *J. Am. Chem. Soc.* **1985**, *107*, 1701.  
 (11) For a description of the Cambridge Structural Database and studies based on it see: (a) Allen, F. H.; Bellard, S.; Brice, M. D.; Cartwright, B. A.; Doubleday, A.; Higgs, H.; Hummelink, T.; Hummelink-Peters, B. G.; Kennard, O.; Motherwell, W. D. S.; Rogers, J. R.; Watson, D. G. *Acta Crystallogr., Sect. B* **1973**, *35*, 2331. (b) Allen, F. H.; Kennard, O.; Taylor, R. *Acc. Chem. Res.* **1983**, *16*, 146.  
 (12) (a) Gilli, G.; Bellucci, F.; Ferretti, V.; Bertolasi, V. *J. Am. Chem. Soc.* **1989**, *111*, 1023.  
 (13) (a) Bürgi, H.-B. *Angew. Chem., Int. Ed. Engl.* **1975**, *14*, 460. (b) Dunitz, J. D. *X-ray Analysis and the Structure of Organic Molecules*; Cornell University Press: Ithaca, NY, 1979. (c) Murray-Rust, P.; Bürgi, H. B.; Dunitz, J. D. *Acta Crystallogr.* **1979**, *A35*, 703. (d) Bürgi, H.-B.; Dunitz, J. D. *Acc. Chem. Res.* **1983**, *16*, 153.

- (13) (a) McGarrity, J. F.; Cretton, A.; Pinkerton, A. A.; Schwarzenbach, D.; Flack, H. D. *Angew. Chem. Suppl.* **1983**, 551; *Angew. Chem., Int. Ed. Engl.* **1983**, *22*, 405. (b) Pratt, D. V.; Hopkins, P. B. *J. Am. Chem. Soc.* **1987**, *109*, 5553.  
 (14) For a review on helical compounds and molecular propellers see: (a) Meurer, K. P.; Vogtle, F. *Top. Curr. Chem.* **1985**, *127*, 1. (b) Willem, R.; Gielen, M.; Hoogzand, C.; Pepermans, H. In *Advances in Dynamic Stereochemistry*; Gielen, M., Ed.; Freund: London, 1985; p 207. (c) Mislow, K. *Acc. Chem. Res.* **1976**, *9*, 26.

**Table I.** Selected Experimental (X-ray) and Calculated (MM2(85)) Bond Lengths (Å) for Enols **1a–e** and Ethylene **4**


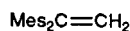
compd	C=C		C—O		=C—Ar( $\beta$ )		=C—Ar( $\beta'$ )		=C—R	
	calcd	exptl	calcd	exptl	calcd	exptl	calcd	exptl	calcd	exptl
<b>1a</b> (anti)	1.349	1.339 (9) 1.31 (1) 1.334 (8) 1.320 (8)	1.360	1.375 (9) 1.370 (9) 1.364 (8) 1.377 (7)	1.494	1.503 (9) 1.49 (1) 1.500 (9) 1.512 (9)	1.497	1.486 (9) 1.51 (1) 1.498 (9) 1.530 (8)		
<b>1a</b> (syn)	1.349		1.359		1.495		1.498			
<b>1b</b> (anti)	1.352	1.311 (8)	1.363	1.371 (8)	1.498	1.492 (8)	1.500	1.515 (9)	1.512	1.51 (1)
<b>1b</b> (syn)	1.351		1.364		1.500		1.500		1.512	
<b>1c</b> (syn)	1.353	1.329 (9) 1.339 (7)	1.364	1.371 (7) 1.390 (8)	1.500	1.511 (8) 1.49 (1)	1.500	1.500 (7) 1.514 (7)	1.518	1.49 (1) 1.499 (7)
<b>1d</b> (syn)	1.355	1.359 (8)	1.364	1.371 (7)	1.499	1.505 (8)	1.502	1.493 (8)	1.524	1.494 (8)
<b>1d</b> (anti)	1.354		1.364		1.499		1.502		1.523	
<b>1e</b> (syn)	1.356	1.350 (5)	1.367	1.391 (4)	1.500	1.511 (4)	1.507	1.516 (3)	1.541	1.519 (4)
<b>4</b>	1.348	1.31 (1)			1.494	1.499 (8)	1.494	1.514 (8)		

**Figure 3.** Stereoscopic view of **1c**.**Figure 4.** Stereoscopic view of **1d**.**Figure 5.** Stereoscopic view of **1e**.

ment of the diarylviny1 moiety in all known solid-state structures containing it. In addition, since Bürgi and Dunitz have shown that analysis of crystal data sometimes allows the mapping of minimum energy rotational (as well as reaction) pathways,<sup>12</sup> we decided to analyze the crystal structures of all molecules containing the diarylviny1 moiety, in order to see how general is the dichotomy of rotational mechanisms observed experimentally for **1a/1b–e**.<sup>5a,b</sup> The results of similar analysis for benzophenones and 1,2-diarylviny1 systems will be reported shortly.

## Results and Discussion

**Structural Commentary.** Enols **1a–e** were prepared according to Fuson and co-workers<sup>15a,b</sup> or as described by us previously.<sup>15c</sup> Single crystals were grown from a dilute solution of hexane (for **1a**) or ethanol (for **1b–e**). For evaluating the effect of the OH group on the torsional angle, we also determined the structure of 1,1-dimesitylethylene (**4**), the parent substrate for our 2,2-



4

(15) (a) Enol **1a**: Fuson, R. C.; Armstrong, L. J.; Kneisley, J. W.; Shenk, W. J. *J. Am. Chem. Soc.* **1944**, *66*, 1464. See also: Reference 6a. (b) **1b**: Fuson, R. C.; Armstrong, L. J.; Chadwick, D. H.; Kneisley, J. W.; Rowland, S. P.; Shenk, W. J.; Sofer, Q. F. *J. Am. Chem. Soc.* **1945**, *67*, 386. (c) **1c–e**: Reference 3.

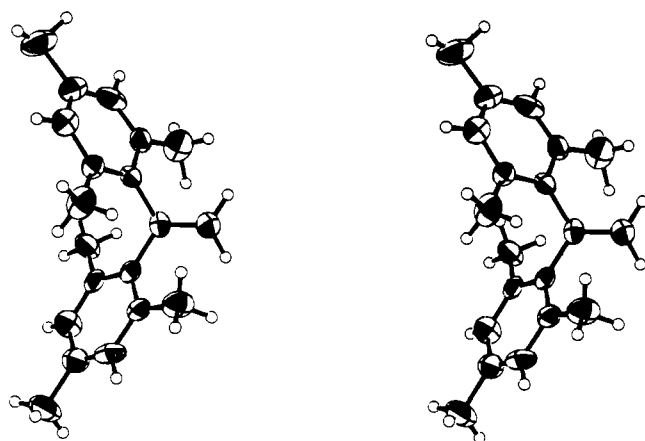
(16) Ethylene **4** was prepared according to: Roberts, R. M.; El-Khawaga, A. M.; Roengsumram, S. *J. Org. Chem.* **1984**, *49*, 3180.

**Table II.** Selected Calculated and Experimental Bond Angles (deg) for *syn*- or *anti*-**1a–e** and **4**

compd	$\alpha_1$		$\alpha_2$		$\alpha_3$		$\alpha_4$		$\alpha_5$		$\alpha_6$	
	exptl	calcd	exptl	calcd	exptl	calcd	exptl	calcd	exptl	calcd	exptl	calcd
<b>1a</b>	117.9 (6)	120.3	120.6 (6)	120.8	121.5 (6)	118.9	118.0 (7)	120.1	119.5 (7)	114.8	122.4 (6)	125.1
	117.5 (6)		122.9 (6)		119.6 (6)		116.9 (8)		117.7 (8)		125.4 (7)	
	116.3 (6)		122.8 (5)		120.9 (6)		118.9 (7)		119.2 (7)		121.9 (6)	
	120.6 (5)		117.9 (5)		121.4 (5)		118.6 (7)		118.4 (6)		123.0 (6)	
	118.1 <sup>a</sup>		121.0 <sup>a</sup>		120.8 <sup>a</sup>		118.1 <sup>a</sup>		118.7 <sup>a</sup>		123.7 <sup>a</sup>	
<b>1b</b>	121.8 (4)	121.9	118.2 (4)	119.6	119.9 (4)	118.8	126.0 (6)	123.6	112.4 (5)	114.0	121.6 (5)	122.8
<b>1c</b>	120.1 (5)	122.5	119.9 (4)	119.5	119.9 (4)	117.8	127.0 (5)	123.7	109.0 (5)	114.2	123.8 (5)	121.8
	119.7 (5)		121.3 (5)		119.0 (4)		127.7 (5)		109.1 (5)		123.0 (6)	
	119.9 <sup>b</sup>		120.6 <sup>b</sup>		119.4 <sup>b</sup>		127.4 <sup>b</sup>		109.0 <sup>b</sup>		123.4 <sup>b</sup>	
<b>1d</b>	120.4 (5)	122.6	121.2 (5)	119.1	118.4 (5)	118.1	127.7 (5)	123.8	110.0 (2)	114.5	121.8 (5)	121.6
<b>1e</b>	125.4 (3)	125.4	116.3 (2)	117.3	118.3 (2)	117.3	133.2 (3)	128.1	107.4 (2)	112.6	119.2 (3)	119.0
<b>4</b>	120.6 (6)	119.8	117.3 (5)	120.6	122.0 (6)	119.8	120.0 (5)	121.8	118.3 (6)	116.4	121.5 (7)	121.8

<sup>a</sup> Average of the values for the four crystallographic forms of **1a**. <sup>b</sup> Average of the values for the two crystallographic forms of **1c**.**Table III.** Important Intramolecular Nonbonded Distances (Å)<sup>a</sup>

	<b>1a</b>				<b>1b</b>	<b>1c</b>		<b>1d</b>	<b>1e</b>	<b>4</b>
	A	B	C	D		A	B			
C(2)–A	3.068	2.981	3.027	3.039	3.024	3.014	2.978	3.016	2.975	3.001
C(2)–B	2.986	3.026	2.999	2.997	2.962	2.990	3.010	2.969	3.030	3.001
C(2)–C	2.973	2.960	2.979	2.971	3.032	2.996	2.998	2.954	3.002	2.994
C(2)–D	2.980	3.008	2.990	2.986	2.995	3.018	3.008	3.033	3.028	2.993
A–C	3.984	3.665	3.653	3.761	3.548	3.467	3.584	3.384	3.378	3.776
B–D	3.610	3.765	3.660	3.524	3.563	3.525	3.613	3.396	3.282	3.645
C(3)–HO <sup>b</sup>						2.463	2.420	2.348	2.177	
C(8)–HO <sup>b</sup>						2.597	2.640	2.512	2.468	
C(4)–HO <sup>b</sup>						3.348	3.325	3.225	3.007	

<sup>a</sup> For labeling of methyls A–D, see structure 5. <sup>b</sup> Distance between the aromatic carbon and the enolic hydrogen.**Figure 6.** Stereoscopic view of **4**.

designated H(11) and H(12). For 2,2-dimesityl-ethanol (**1a**) there are four crystallographically independent molecules in the asymmetric unit, forming tetramers held by hydrogen bonds between the hydroxyl groups. The unit cell packing diagrams of **1a** is shown in Figure S1 (supplementary material). 1,1-Dimesitylpropen-2-ol (**1b**) crystallizes with solvent molecules (ethanol). The crystals are unstable and tend to lose solvent molecules. The crystal was therefore analyzed after it was introduced into a sealed walled capillary. The ethanol molecules are linked by hydrogen bonds to two enol molecules related by an inversion center, thus forming a "tetrameric" like hydrogen-bonding scheme involving two enol and two solvent molecules. The packing diagram is given in Figure S2 (supplementary material). For 1,1-dimesityl-1-buten-2-ol (**1c**) there are 2 crystallographically independent molecules in the asymmetric unit.

Crystallographic data are summarized in the Experimental Section, and selected bond lengths and angles are given in Tables I and II, which include also the MM2(85) calculations of the *syn* and *anti* geometries of the C=C–OH moiety. In all the cases calculated, the energies and geometries (excluding that of the OH) are similar for both conformations (Table I). Interesting nonbonded distances between the *o*-methyl groups of the mesityl rings

and C(2) or the *o*-methyl groups on a different ring but on the same face of the double bond, and between the enolic hydrogen and the carbons of the mesityl ring *cis* to it, are given in Table III. A complete list of the experimental bond lengths and angles, positional parameters, thermal parameters, and structure factors are given in Tables S1–S30 (supplementary material).

**Geometrical Parameters.** All six structures were refined to relatively large *R* values, and therefore the significance of very small variations in bond lengths and angles is not clear. However, general features are mentioned below.

(a) **C=C Bond Lengths.** We have shown previously that enols **2** display C=C bond lengths of 1.339–1.362 Å. In the series of **1a–e** the C=C bond lengths range from 1.31 Å (for one of the four crystallographically independent molecules of **1a**) to 1.359 Å (for **1d**). In general, the experimental data display a trend of longer C=C bonds with the increase of bulk of R<sup>1</sup>.<sup>17</sup> The C=C bond length for **4** is 1.31 Å, being identical with that in one of the independent molecules of **1a**, indicating that the introduction of an OH group to the dimesitylvinyl moiety does not lead to an elongation of the C=C bond by either steric or resonance (i.e., Mes<sub>2</sub>CC(R<sup>1</sup>)=OH) effects. The MM2(85) calculations<sup>18</sup> do reproduce the experimental trend: The longer calculated C=C bonds (1.35 and 1.36 Å) correspond to the more sterically crowded molecules **1d** and **1e**. However, the bond lengths of the less crowded members (**1a–c**, **4**) are overestimated by the calculations.

(b) **C–O Bond Lengths.** The C–O bond length is not very sensitive to a change in R<sup>1</sup>, except that it is the longest (if the experimental error is neglected) when R<sup>1</sup> = *t*-Bu. The calculated data show an increase in the C–O bond length with the increased bulk of R<sup>1</sup>. However, all the C–O bond lengths are severely underestimated.

(c) **C–Ar Bond Lengths.** The C–Ar bond lengths range from 1.49 (1) to 1.514 (8) Å. Although the calculation predicts an elongation of these bonds with the increase of bulk of R<sup>1</sup>, no clear experimental trend is observed.

(17) It should be noted that although **1d** displays an experimentally longer C=C bond than **1e**, these two bonds are identical within the experimental error.

(18) Allinger, N. L. *QCPE* MM2(85). See also: Sprague, J. T.; Tai, J. C.; Yuh, Y. H.; Allinger, N. L. *J. Comput. Chem.* **1987**, *8*, 581.

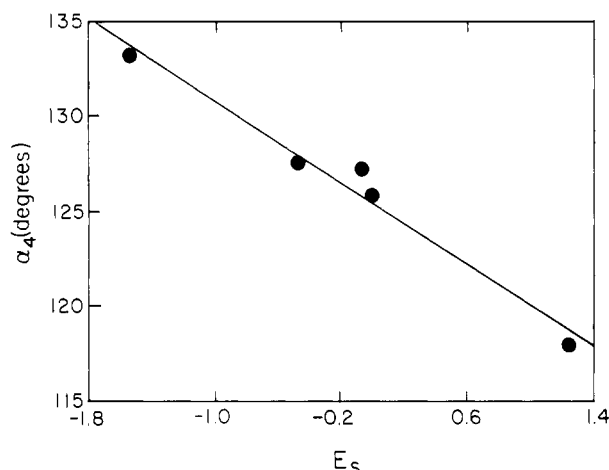
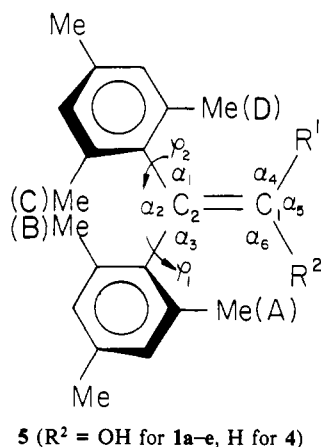


Figure 7. Plot of  $\alpha_4$  for **1a–e** vs Taft's steric parameters  $E_s$ .

**(d) Bond Angles.** In general the bond angles (see notation in **5**) around the C=C bond are affected by the bulk of  $R^1$ :  $\alpha_1$  and  $\alpha_4$  increase with the bulk of R whereas  $\alpha_2$ ,  $\alpha_3$ ,  $\alpha_5$ , and  $\alpha_6$  decrease.

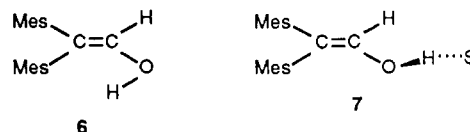


The changes are not to the same extent: The angles  $\alpha_4$  and  $\alpha_5$  involving  $R^1$  are the most affected, whereas angle  $\alpha_3$  is the least affected. For the enols,  $\alpha_4$  opens from an average value of  $118.1^\circ$  to  $133.2^\circ$  for **1e** and  $\alpha_5$  decreases from an average value of  $118.7^\circ$  to  $107.4^\circ$  with the increased bulk of  $R^1$  from H to *t*-Bu. The change from **1c** to **1d** is an exception since it increases  $\alpha_5$ , but this increase is within the experimental error. When these angles (the average value was used for **1a** and **1c**) are plotted against Taft's steric parameter  $E_s$ <sup>19</sup> for  $R^1$ , a linear relationship is obtained (Figure 7). The small changes in the third angle at C(1), i.e.,  $\alpha_6$  are irregular and follow the order **1c** (average) > **1a** (average) > **1d** > **1b** > **1e**. These trends are correctly reproduced by the MM2(85) calculations, although for some angles (e.g.,  $\alpha_5$ ) there are large discrepancies between the calculated and experimental values.

**(e) Torsional Angles.** The agreement between calculated and experimental torsional angles of the rings for **1a–e**<sup>5b</sup> is satisfactory only for  $\phi_2$ . Angle  $\phi_1$  is underestimated especially in the more crowded members of the series.<sup>20</sup>

**(f) Conformation of the Alkyl Group.** The alkyl conformation in **1b–e** is such that one group attached to C(21) is eclipsed with the double bond. It is observed in **1c** and **1d** that the molecules prefer to eclipse one C–H rather than a C–C bond. In enols **1b**, **1c**, and **1d** the C(2)–C(1)–C(21)–H torsional angle is  $0.5^\circ$ ,  $13.6^\circ$ , and  $21.1^\circ$ , respectively, whereas in **1e** one C–Me bond is perfectly eclipsed with the double bond (C(2)–C(1)–C(21)–C(23) =  $0^\circ$ ).

**(g) Hydrogen Bonding.** In our previous investigation of stable simple enols in solution, we have shown by using spectroscopic (NMR, IR) data that the conformation of the OH moiety and the hydrogen-bonding interaction are strongly interrelated.<sup>1b,6</sup> In nonpolar, non hydrogen bond accepting solvents, the conformation is syn (**6**) whereas in solvents (S) of high hydrogen bond accepting



abilities such as DMSO the conformation is anticlinal (**7**) with a C=C–O–H angle  $<150^\circ$ . These differences were rationalized in terms of steric effects. When the solvent is a non hydrogen bond acceptor, the OH proton is intramolecularly hydrogen bonded to the mesityl ring cis to it, whereas when a good hydrogen bond accepting solvent is present, a conformational syn  $\rightarrow$  anti change takes place in order to reduce the steric interactions between the enol and the intermolecularly hydrogen bonded solvent molecule.

Enols **1b–e** conform to this picture. When solvent of crystallization is absent, the conformation is **6**, whereas for the ethanol solvate of **1b** the conformation is **7**, as found earlier for **2b–EtOH**.<sup>9</sup> The torsional C=C–O–H angles are  $172.5^\circ$ ,  $-162.3^\circ$ ,  $161.9^\circ$ , and  $-178.8^\circ$  for the four forms of **1a**,  $178.1^\circ$  for **1b**,  $-5.1^\circ$  and  $7.8^\circ$  for the two forms of **1c**,  $6.5^\circ$  for **1d**, and  $2.7^\circ$  for **1e**. In **1b–EtOH**, the enolic OH is hydrogen bonded to the ethanolic proton and both are hydrogen bonded to another pair related by an inversion center (Figure S2). The O...O distances of 2.683 and 2.837 Å are comparable to the values for **2b–EtOH** (2.627 and 2.675 Å)<sup>9</sup> and in other compounds.<sup>21</sup>

Of special interest is the bonding scheme in **1a**, the less crowded enol of the series. Its hydrogen-bonding scheme involves four molecules in conformation **7** cyclically hydrogen bonded in an arrangement in which the enol molecules serve both as donors and acceptors. Since there are no symmetry relations within the hydrogen-bonding net, the four O...O distances are different: 2.669, 2.712, 2.722, 2.742 Å, all within the range of hydrogen bond. It seems likely that the cyclic intermolecular hydrogen bonding present in **1a** is allowed by the low steric bulk of the  $\alpha$ -hydrogen. It should be noted that whereas hydroxyl groups tend to form hydrogen bonds with strong electronegative groups such as carbonyl and fluorides, few structurally characterized crystal structures involve hydrogen bonding between OH groups.<sup>22</sup>

The distances between the enolic hydrogen and the carbons of the  $\beta'$  ring cis to it are important, since it was shown that short OH–C distances can be taken as an indication of an intramolecular  $\pi$  (Ar)–OH hydrogen bond.<sup>23</sup> For each of the enols **1c–e** existing in the crystal in conformation **6** the shortest OH–C (Ar) distance corresponds to OH–C(3) (Table III). These distances range from 2.463 to 2.177 Å and decrease with the increase of bulk of  $R^1$ , which is associated with the decrease of the bond angle C=C–O  $\alpha_6$  (Table II). The value for **1e**, which is similar to the values (2.11 and 2.16 Å) reported by Schweizer et al.,<sup>23</sup> can be taken as crystallographic evidence for a  $\pi$  (Ar)–OH hydrogen bonding. Although the corresponding distances are longer for **1c** and **1d**, the spectroscopic data in solution suggest that both exist in CCl<sub>4</sub> as intramolecular hydrogen-bonded species.<sup>6b</sup> In summary, enols **1** show three possible hydrogen-bonding arrangements: intramolecular  $\pi$ –OH and intermolecular enol–enol and enol–EtOH bonding.

**(h) Nonbonded Distances.** Two kinds of nonbonded distances are relevant to our discussion: those between the *o*-Me groups and C(2) and inter-ring *o*-Me...*o*-Me distances for methyl groups

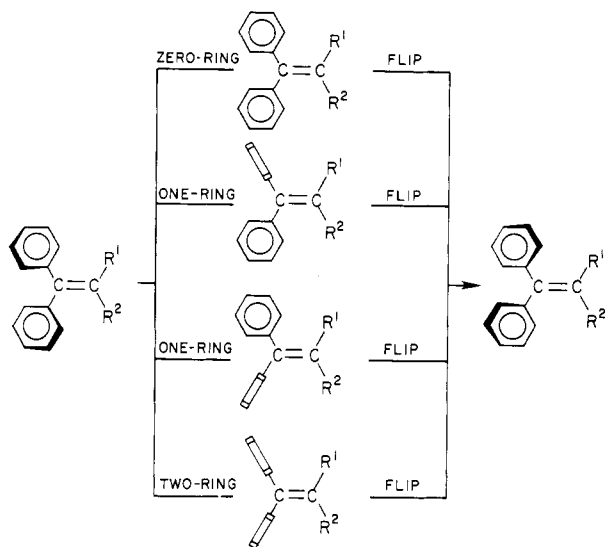
(19) Taft, R. W. In *Steric Effects in Organic Chemistry*; Newman, M. S., Ed.; Wiley: New York, 1956; Chapter 13.

(20) MMP2 calculations of substituted triarylethylenes showed a similar underestimation of the torsional angles of the aryl rings: Duox, W. L.; Griffin, J. F. *J. Steroid Biochem.* **1987**, *27*, 271.

(21) For a review see: Bishop, R.; Dance, I. G. *Top. Curr. Chem.* **1988**, *149*, 137.

(22) Most of the OH–OH hydrogen bonds involve a water molecule. However, several examples exist of OH groups involved in a cyclic hydrogen-bonded arrangement. See, for example: Saenger, W.; Noltemeyer, M.; Manor, P. C.; Hingerty, B.; Klar, B. *Bioorg. Chem.* **1976**, *5*, 187. Andreotti, G. D.; Ungaro, R.; Pochini, A. *J. Chem. Soc., Chem. Comm.* **1979**, 1005.

(23) Schweizer, W. B.; Dunitz, J. D.; Pfund, R. A.; Ramos Tombo, G. M.; Ganter, C. *Helv. Chim. Acta* **1981**, *64*, 2738.



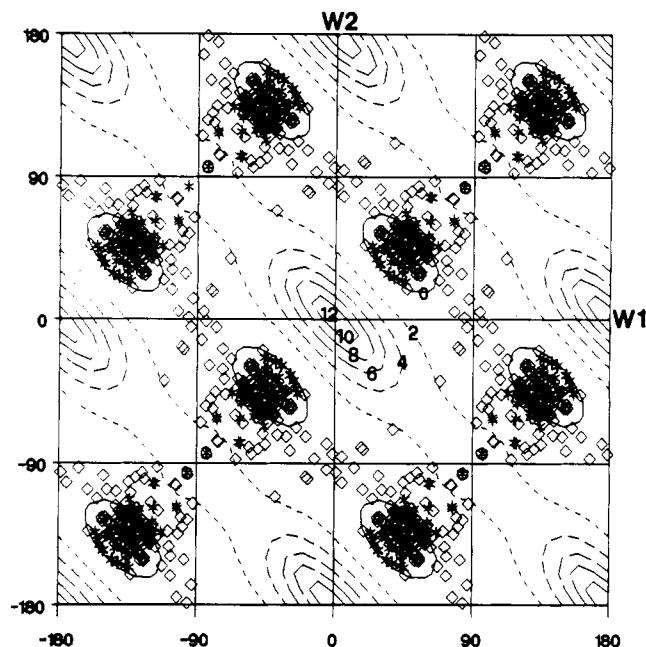
**Figure 8.** Idealized transition states for zero-, one- ( $\beta$  and  $\beta'$ ), and two-ring flips in  $\text{Ar}^1\text{Ar}^2\text{C}=\text{CR}^1\text{R}^2$ . An open rectangle indicates a ring that is perpendicular to the  $\text{C}=\text{C}$  plane.

located on the same side of the double-bond plane. Both should reflect the steric crowding of the dimesitylvinyl moiety and should display different dependence on the aryl torsional angles. Whereas to a first approximation, any  $o\text{-Me}\cdots\text{C}(2)$  distance should be independent of the  $=\text{C}-\text{Ar}$  torsional angle, the  $o\text{-Me}\cdots o\text{-Me}$  distances should change with the torsional angles of the rings: The closer to  $90^\circ$  is the dihedral angle of the rings the shorter are the distances.

The  $o\text{-Me}\cdots\text{C}(2)$  distances are fairly constant and range from 2.954 to 3.039 Å (Table III). Interestingly, enol **2b** showed a somewhat larger spread of distances (2.954–3.071 Å).<sup>9</sup> The  $o\text{-Me}\cdots o\text{-Me}$  distances show a larger spread: from 3.984 Å for one of the independent crystallographic molecules of **1a** to 3.282 Å for **1e**. The  $\beta$   $o\text{-Me}\cdots\beta'$   $o\text{-Me}$  distance for **1e** is the shortest found for any of the enols studied to date. This is in full agreement with the expected trend, since **1e** has the largest torsional angles of the rings of all the 1,1-dimesitylvinyl systems studied so far.

**Correlated Rotation in Diarylethylenes.** Molecular propellers of the type  $\text{Ar}_3\text{X}$ ,  $\text{Ar}_3\text{XY}$ ,  $\text{Ar}_2\text{C}=\text{C}(\text{Y})\text{Ar}$ , and  $\text{Ar}_2\text{C}=\text{C}(\text{X})\text{Y}$  and others display correlated rotation commonly analyzed in terms of “flip” mechanisms,<sup>24</sup> all of which involve helicity reversal. In these mechanisms as applied to the enols (e.g., **2a** and **2b**), the ring that “flips” passes through a plane perpendicular to the double-bond plane, while the remaining rings rotate concurrently in the opposite direction. Depending on the number of flipping rings, these mechanisms are dubbed zero-, one-, two-, or three-ring flip. The idealized transition states for these mechanisms as applied to an  $\text{Ar}_2\text{C}=\text{CR}^1\text{R}^2$  system are schematically depicted in Figure 8.<sup>25</sup> We have previously shown<sup>5a,b</sup> that the rotational mechanism of lowest activation energy (threshold mechanism) in **1a** is the  $\beta'$ -ring flip (a one-ring flip process) whereas for **1b–e** the threshold mechanism is a  $\beta, \beta'$  two-ring flip process. In contrast to this shift in threshold mechanism, for molecular propellers of the types  $\text{Ar}_3\text{X}$ , and  $\text{Ar}_3\text{XY}$  the threshold mechanism is uniformly a two-ring flip.<sup>26,27</sup>

**Conformational Map and Application of the Principle of Structural Correlation for 1,1-Diarylviny Propellers.** The con-



**Figure 9.** Conformational map ( $w_1$  vs  $w_2$ ) for 1,1-diarylviny compounds. The contours are calculated equipotential energy regions for  $\text{Ph}_2\text{C}=\text{CH}_2$  where the numbers denote the energies in kilocalories per mole. The points are for  $\phi_1, \phi_2$  of  $\text{Ar}_2\text{C}=\text{CR}^1\text{R}^2$  from Table S31; ( $\diamond$ )  $\text{R}^1 \neq \text{R}^2$ ; ( $*$ )  $\text{R}^1 = \text{R}^2$ ; ( $\odot$ ) compound **10**, Table S31.

formation of a diarylviny moiety can be described by the two torsional angles of the aryl groups with the double-bond plane ( $\phi_1$  and  $\phi_2$ ).  $\phi$  values of  $0^\circ$  and  $90^\circ$  correspond respectively to situations in which the ring is coplanar with the double-bond plane or perpendicular to it. In order to plot the energy changes as a function of the rotational angle of the aryl rings, it is useful to describe the system by a *conformational map* in which the internal energy is plotted as a function of the torsional angles of the rings. This conformational map of coordinates ranging from zero to  $2\pi$  may be considered as a finite part of an infinite two-dimensional lattice (in which each coordinate ranges from  $-\infty$  to  $+\infty$ ) in the same way that a unit cell forms part of an infinite three-dimensional lattice in crystallography.<sup>28</sup> The symmetry properties of the potential energy surface can be described in terms of two-dimensional space groups resulting from the symmetry of the nonrigid molecule (which may be expressed by the Longuet-Higgins molecular symmetry group (MSG) of feasible permutations). In these space groups a set of equivalent “general positions” corresponds to a set of isometric<sup>29</sup> conformations, and its special positions correspond to structures having higher symmetry.<sup>28</sup>

**Molecular Symmetry Group.** The molecular symmetry group of an  $\text{Ar}_2\text{C}=\text{CH}_2$  molecule is identical with the MSG of an  $\text{Ar}_2\text{CH}_2$  molecule, analyzed by Dunitz<sup>12b,c</sup> in which all distinct isometric conformations possible can be mapped in  $1/16$ th of the  $180^\circ \times 180^\circ$  conformational space (the “asymmetric unit”). The full symmetry operations of this group on the twist angles produce a set of rotational angles ( $w_1$  and  $w_2$ ) related by symmetry in a two-dimensional conformational map, which may be referred to the plane group *cmm* by setting the translation vectors  $S_1 = t_1$  (along  $w_1$ ) +  $t_2$  (along  $w_2$ ) and  $S_2 = -t_1 + t_2$ . For the new unit cell four isometric conformations exist for a general position,  $p(\phi_1, \phi_2)$ .<sup>30</sup>

(24) Kurland, R. J.; Schuster, I. I.; Colter, A. K. *J. Am. Chem. Soc.* **1965**, *87*, 2279.

(25) We use the term “idealized” since there is no evidence that the  $\phi$ 's of the rings are exactly  $0^\circ$  or  $90^\circ$  in the various transition states, or even that the rings are planar (cf. discussion below and Figure 10D,E).

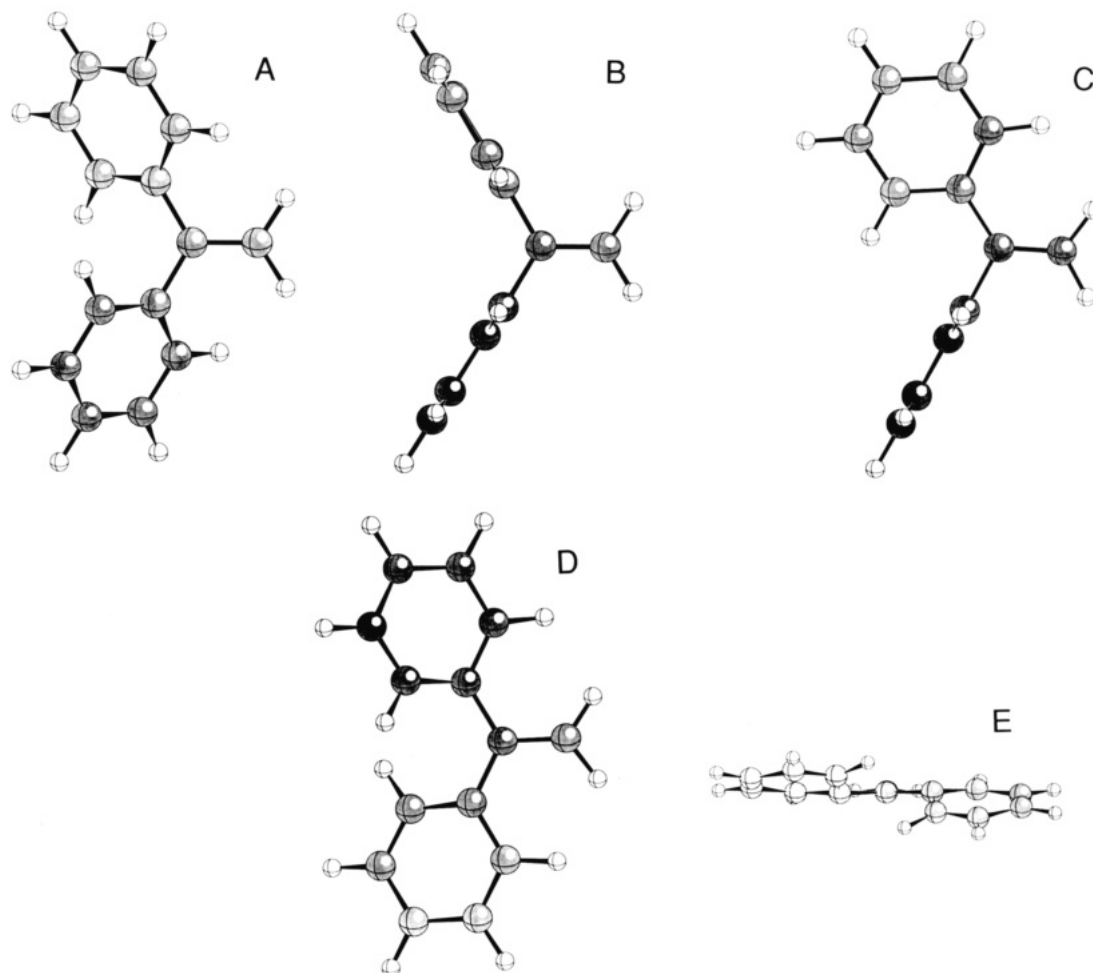
(26) (a) Hummel, J. P.; Gust, D.; Mislow, K. *J. Am. Chem. Soc.* **1974**, *96*, 3679. Wille, E. E.; Stephenson, D. S.; Capriel, P.; Binsch, G. *Ibid.* **1982**, *104*, 405. (b) Andose, J. D.; Mislow, K. *Ibid.* **1974**, *96*, 2168.

(27) (a) Bye, E.; Schweizer, W. B.; Dunitz, J. D. *J. Am. Chem. Soc.* **1982**, *104*, 405. (b) Clegg, W.; Lockart, J. C. *J. Chem. Soc., Perkin Trans. 2* **1987**, 1621.

(28) For a discussion and descriptions of conformational maps see: Reference 12b, Chapter 10.

(29) Two structures are isometric if they are properly or improperly congruent. See: Anet, F. A. L.; Miura, S. S.; Siegel, J.; Mislow, K. *J. Am. Chem. Soc.* **1983**, *105*, 1419, footnotes 3 and 4.

(30) The general and special positions of the plane group *cmm* can be found in standard works, for example in the: *International Tables for X-ray Crystallography*, 1st ed; Kynoch Press: Birmingham, England, 1952; Vol. 1.



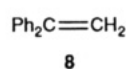
**Figure 10.** Calculated (MM2(85)) conformations of the lower energy form (A) and the transition states (viewed from a normal to the C=C plane) for the two-ring flip (B), the one-ring flip (C), and zero-ring flip (D) (also viewed along the C=C bond (E)) of 1,1-diphenylethylene.

**Table IV.** Calculated Structural Parameters for the Ground-State and Rotational Transition States of 1,1-Diphenylethylene<sup>a</sup>

parameter <sup>a</sup>	ground state	transition state for <i>n</i> -ring flip			
		zero-ring	one-ring	two-ring	C <sub>2v</sub> <sup>b</sup>
C(1)–C(2)	1.349	1.358	1.348	1.340	1.363
α <sub>1</sub>	120.4	118.8	115.6	120.8	115.2
α <sub>2</sub>	119.3	122.4	119.4	118.4	129.5
α <sub>3</sub>	120.4	118.7	124.9	120.8	115.2
C(2)–C(3)–C(4)	121.4	123.2	122.9	120.1	122.2
C(2)–C(3)–C(8)	120.0	119.8	119.8	120.0	126.5
C(2)–C(12)–C(13)	120.0	119.3	120.2	120.1	126.5
C(2)–C(12)–C(17)	121.4	123.4	120.0	120.0	122.2
C(1)–C(2)–C(12)–C(13)	140	154 <sup>c</sup>	180	90	180
C(1)–C(2)–C(3)–C(8)	140	153 <sup>d</sup>	90	90	180

<sup>a</sup> Bond lengths in angstroms, angles in degrees. <sup>b</sup> Planar structure of C<sub>2v</sub> symmetry (see text). <sup>c</sup> C(1)–C(2)–C(12)–C(17) = 0°. <sup>d</sup> C(1)–C(2)–C(3)–C(4) = 0°.

**Molecular Mechanics Calculations.** In an early study, Stegemeyer and Rapp<sup>31a</sup> calculated the potential energy of 1,1-diphenylethylene (**8**) as a function of the torsional angles of the rings. More recently, Baraldi et al. calculated the conformational energy map of **8** using the C-INDO method.<sup>31b</sup> We recalculated the potential energy map for the rotation of **8**, using state of the art



molecular mechanics calculations (the MM2(85) program). The calculations were performed by driving the Ar–C=C torsional

angle of one of the rings from 0° to 180° and that of the other ring from 0° to 90°, using in each case 10° increments. The resulting 10 × 19 matrix did not have the proper symmetry in several regions, and the calculations were therefore repeated in these areas, driving the ring in the opposite direction, affording self-consistent results. The calculated energies are plotted in the form of a contour map in Figure 9.

Several conclusions can be extracted from the map: (a) The region of lowest calculated energy corresponds to  $\phi_1 = \phi_2 = 40^\circ$ , i.e., a propeller conformation where the two rings are twisted in the same sense. This conformation represents a compromise between the resonance interaction (highest when the rings are coplanar with the double bond) and the steric interaction. (b) The region in which the two rings tend to be coplanar with the double bond ( $\phi < 10^\circ$ ) has the highest energy. (c) Enantiomerization (helicity reversal) of the molecule should occur through

(31) (a) Stegemeyer, H.; Rapp, W. *Ber. Bunsen-Ges. Phys. Chem.* **1971**, *75*, 1165. (b) Baraldi, I.; Gallinella, E.; Momicchioli, F. *J. Chim. Phys.* **1986**, *83*, 653.



correlated rotation by a one-ring flip process with a barrier of 1.2 kcal mol<sup>-1</sup>. Another process slightly higher in energy involves a two-ring flip process: The calculated transition states for the two-, one-, and zero-ring flips lie 3.0, 1.2, and 12.9 kcal mol<sup>-1</sup> above the low-energy conformation and have approximately  $C_{2v}$ ,  $C_s$ , and  $C_2$  symmetries, respectively. The calculated geometries for the different transition states are shown in Figure 10, and selected structural parameters are collected in Table IV. The calculated geometries are normal except in one case which is of special interest. In the calculated structure of the transition state of the zero-ring flip, the molecule adopts an helical  $C_2$  structure in which the ortho carbons are displaced from the double-bond plane in opposite directions in order to alleviate the steric interactions between the two rings. These distortions of the aryl rings from planarity are appreciable: Whereas the C(1)–C(2)–C(12)–C(17) and C(1)–C(2)–C(3)–C(4) torsional angles are 0°, the C(1)–C(2)–C(12)–C(13) and C(1)–C(2)–C(3)–C(8) torsional angles are ca. 154° and the puckerings are clearly displayed in Figure 10E. The energy gain by this distortion is estimated by calculating a planar  $C_{2v}$  structure, which was found to lie 5.6 kcal mol<sup>-1</sup> above the transition state for the zero-ring flip.

In general, the barriers are lower than those (6.5, 3.9, and ≥100 kcal mol<sup>-1</sup>, respectively) calculated by Stegenmeyer and Rapp<sup>31a</sup> and are similar to those calculated by Baraldi et al. (2.9, 1.8, >10 kcal mol<sup>-1</sup>)<sup>31b</sup> for the same processes. However, the three calculations indicate that the threshold mechanism for **8** is a one-ring flip, with the two-ring flip lying ca. 2 kcal mol<sup>-1</sup> above it. At present, no experimental rotational barrier is available for **8**, but from NMR studies it must be lower than 10 kcal mol<sup>-1</sup>.<sup>32</sup>

**Application of the Principle of Structural Correlation.** The principle of structural correlation<sup>12</sup> first enunciated by Bürgi and Dunitz, states "if a correlation can be found between two or more independent parameters describing the structure of a given molecular fragment in various environments, then the correlation function maps a minimum energy path in the corresponding parameter space". In recent years, this principle was extensively used for the determination of stereoisomerization and reaction pathways.<sup>33</sup> Its application to our system is as follows: In all molecules of general structure  $Ar^1Ar^2C=CR^1R^2$  whose structures are known from X-ray diffraction, the different substituents are viewed as "perturbations" leading to a distortion of the torsional angles  $\phi_1$  and  $\phi_2$  from their ideal value for **8** in the gas phase. Each X-ray structure is represented in the conformational map of  $\phi_1$  vs  $\phi_2$  by a point. These points should concentrate in low potential energy regions and become less dense in higher potential energy areas. Pathways connecting clusters in the conformational map should represent the minimum energy path for the stereoisomerization.

**Structures of Compounds Used for Data Points.** A search in the Cambridge Crystallographic Database (CSD)<sup>10</sup> for the structural unit  $Ar^1Ar^2C=CR^1R^2$  together with some additional new data yielded 80 different compounds. In some cases there was more than one crystallographically independent molecule (cim) in the asymmetric unit. Hence, the whole data set studied included 126 data points, including 10 from the present work.

The data for all the 1,1-diarylethylenes studied to date by X-ray crystallography are collected in Table S31 (supplementary material), which includes the structures, C=C bond lengths, and bond and torsional angles for 52 compounds with 77 cim. Curiously, in all cases  $Ar^1 = Ar^2$  and in most of them  $Ar = Ph$ . More than 30 triaryl- or tetraarylethylene systems were retrieved, but those showing disorder or an *R* factor >0.10 were excluded. We had previously tabulated<sup>9</sup> 21 compounds with 23 cim (Tables I and

III in ref 9).<sup>34</sup> These data are now complemented in Table S32 (supplementary material), which lists additional 10 compounds (13 cim). In the triarylethylene series there are compounds with  $Ar^1 \neq Ar^2$ .

A formal subdivision of our compounds is to five families: (a) 1,1-diaryl-substituted systems ( $Ar \neq Mes$ ), which include constitutionally "completely symmetric" (i.e.,  $Ar_2C=CR_2$  in which the two vinylic substituents *R* are identical) systems (21 compounds, 32 cim); (b) "apparently symmetric" structures where  $R^1 \neq R^2$ , but  $R^1$  and  $R^2$  are sterically similar at the vicinity of the two aryl groups (four compounds, 6 cim); (c)  $R^1 \neq R^2$ , when the two aryl groups are exposed to different steric environments (28 compounds, 39 cim); (d) triaryl-substituted ethylenes and tetraphenylethylene ( $Ar \neq Mes$ ) (20 compounds, 27 cim); (e) mesityl-substituted systems, which include **1a–e** and **4** (10 cim), eight di- or trimesitylvinyl-substituted systems (9 cim) and tetramesitylethylene (one structure). Although families d and e should preferably be displayed on a three- or four-dimensional map since the torsional angles of all rings should be taken into account, they are included for convenience in the conformational maps of families a–c.

Of all the 1,1-diarylethylenes studied, only compounds of group a can (but not must) display crystallographic  $C_2$  symmetry. It should be noted that if only molecules of  $C_2$  symmetry are studied, the symmetry constraint of the sampling will cause concentration of the points along the (0°, 0°) to (90°, 90°) diagonal, which represent the zero- or the two-ring flip mechanism, whereas the one-ring flip ( $C_s$  point group symmetry) will not be mapped. Consequently, systems lacking  $C_2$  symmetry must be sampled in order to derive the rotational mechanism since only for them the removal of symmetry constraints can allow the mapping of all possibilities.

**Crystal Lattice Forces and Torsional Angles.** In every crystallographic structural study, there is the question of the influence of crystal packing forces on the molecular structure. In the present case examination of Tables S31 and S32 shows that some of the compounds exist in two or more different crystal forms (shown by numbers followed by a suffix) or in two (or more) nonsymmetry-related forms in the crystal. These structures enable estimation of the contribution of packing forces to the torsional angles of the diarylvinyl moiety. Although the lattice effects are mostly not large, sometimes they can be appreciable. For example, the two crystallographic forms of  $Ph_2C=C=C=CPh_2Fe(CO)_4$  (Table S31, entries 15a and 15b) differ in the torsional angle of one ring by >12°.

The C=C bond length and the ArCAr bond angle ( $\alpha_2$ ) are influenced by the presence of substituents. For 79 cim having the 1,1-diarylvinyl moiety the average C=C bond length is  $1.344 \pm 0.014$  Å and  $\alpha_2 = 117.2 \pm 2.2^\circ$ . In the triarylvinyl systems, the average bond length is  $1.344 \pm 0.012$  Å when a single deviating bond length<sup>9</sup> is excluded and the  $\alpha_2$  value is  $115.2 \pm 1.7^\circ$ . We conclude that the bond lengths in the diaryl- and triarylvinyl systems are practically identical whereas  $\alpha_2$  is smaller in the latter. The histograms of the C=C bond lengths for the 1,1-diarylethylenes and for the triarylvinyl derivatives (Figures S3 and S4 (supplementary material) look almost identical).

**Intrinsic Torsional Angles of a 1,1-Diarylvinyl Moiety.** It is noteworthy that except for four 1,1-diarylvinyl systems (entries 33a, 47, 49, and 52b in Table S31; **9–12**, respectively, in Chart I) all the diarylvinyl moieties in di- and triarylvinyl systems (Table S32) appear in a propeller conformation. Three of the exceptions are organometallic derivatives of which **12** has another (propeller) conformation. With heptaphenyl tetra-radialene (entry 33a), one of the  $Ph_2C=$  moieties is a nonpropeller. The reason for this is unknown. Since the "propeller" conformation is found in >100 different crystallographically independent molecules, each with its own substitution pattern and crystal environment, it is a strong indication that the propeller arrangement represents the minimum energy conformation of the 1,1-diarylvinyl moiety.

(32) It has been shown in a study of substituted 1,1-diarylethylenes that none show any indication of restricted rotation in the <sup>1</sup>H NMR spectrum down to -90 °C. Rabinovitz, M.; Agranat, I.; Bergmann, E. D. *Isr. J. Chem.* **1969**, *7*, 795.

(33) See for example: (a) Nachbar, R. B., Jr.; Johnson, C. A.; Mislow, K. *J. Org. Chem.* **1982**, *47*, 4829. (b) Chandrasekhar, K.; Bürgi, H.-B. *J. Am. Chem. Soc.* **1983**, *105*, 7081. (c) Jones, P. G.; Kirby, A. J. *Ibid.* **1984**, *106*, 6207. (d) Kanagasabapathy, V. M.; Sawyer, J. F.; Tidwell, T. T. *Ibid.* **1985**, *50*, 503. (e) Cosse-Barbi, A.; Dubois, J.-E. *Ibid.* **1987**, *109*, 1503.

(34) Please note that the convention used in ref 9 for the designation of  $\phi_1$  and  $\phi_2$  differs from that used here in that  $\phi_1$  and  $\phi_2$  should be exchanged.

The torsional angles of the rings in these propellers are strongly influenced by the double-bond substituents. The smaller angles are expected to be found in the least sterically hindered systems where  $R^1 = R^2 = H$ , but it is still interesting to estimate the "intrinsic" torsional angles for a hypothetical diphenylvinyl moiety with no substituents on C(1). We have recently argued that crowded diarylketenes could be taken as models for estimation of intrinsic torsional angles of the aryl rings.<sup>35</sup> For example, for two 1,1-dimesitylketenes these angles are ca 50°. Unfortunately, the crystal structure of diphenylketene is not available, and other compounds should be used as models. One attractive possibility is  $\text{Ph}_2\text{C}=\text{C}=\text{C}=\text{CPh}_2$  (entries 14a-d, Table S31) where the nearly linear arrangement of the butatriene carbons disallow mutual steric interactions between the two  $\text{Ph}_2\text{C}=\text{C}$  moieties. For this compound torsional angles of 27°, 38.6°, 29.3°, and 35.0° were observed.<sup>36</sup> Disregarding lattice forces, and assuming that the preferred conformation has  $D_2$  symmetry, we estimated an intrinsic torsional angle of ca 32° for a 1,1-diphenylvinyl propeller by averaging the four experimental angles. Notwithstanding the crudeness of the treatment, it is clear that replacement of the phenyls by mesityls results in an appreciable increase (from 32° to 50°) in the torsional angles.

**Crystal Structure Correlation Maps.** Experimental points for all the substituted 1,1-diarylethylene fragments are superimposed on the MM calculated potential energy surface for 1,1-diphenylethylene **8** in Figure 9 as a  $w_1$  vs  $w_2$  map. The diamonds represent 1,1-diarylethylene fragments with  $R^1 = R^2$  and  $\text{Ar} \neq \text{Mes}$ , and the stars represent systems where C(1) is symmetrically substituted ( $R^1 = R^2$ ). Several features are clearly indicated by the map.

(a) An immediately visible feature is that many points belonging to families a-c concentrate at the region of the calculated minimum at (40°, 40°). The correspondence between the calculated surface for **8**, and the preferred solid-state geometry of many molecules containing more hindered fragments, supports the qualitative use of the calculated surface for **8** as a guide for the dynamic behavior of more hindered 1,1-diarylethylenes.

(b) Another clearly visible feature is that the high-energy region around the (0°, 0°) region extending approximately from -30° to +30° in the  $w_1$  and  $w_2$  axes is completely uninhabited even by a single point. Consequently, rotation occurring by a zero ring flip (passing via the (0°, 0°) region) is highly unlikely.

(c) There is an extensive clustering of the points along the valley represented by the (0°, 90°); (90°, 0°) diagonal, with a few points close to its extreme ends. Most of the points that set this trend indeed belong to the "asymmetric" family c, i.e., when  $R^1 \neq R^2$ . The map of unsymmetrical structures shows much more promise as a probe for the dynamics of the system. This is demonstrated in Figure S5 (supplementary material), which shows a conformational map for two subgroups of compounds. (i) Allene and butatriene derivatives (squares in Figure S5), where steric interference from the C(1) substituents is minimal, cluster around the minimum of the (0°, 90°); (90°, 0°) diagonal. (ii) Compounds with  $R^1 = H$  and  $R^2 \neq H$ , where the difference in steric environment around the two aryl groups is at a maximum and the aryl groups are not ortho-substituted (stars in figure S5), are spread along the (0°, 90°); (90°, 0°) diagonal. Consequently, the crystal structure correlation principle suggests that the one-ring flip is a likely rotational mechanism for unsymmetrical 1,1-diarylviny propellers especially when  $R^1 = H$  and the aryl rings are not ortho-substituted.

There are points along the other diagonal (0°, 0°); (90°, 90°), between the (40°, 40°) minimum and the (90°, 90°) region. An extreme case is an ortho-substituted system (2-HO-3-O<sub>2</sub>N-5-ClC<sub>6</sub>H<sub>2</sub>)<sub>2</sub>C=CCL<sub>2</sub> (item 10 in Table S31, circle in Figure 9) where both rings are almost perpendicular to the double-bond plane ( $\phi_1 = \phi_2 = 83.7^\circ$ ). Points belonging to this group include many of

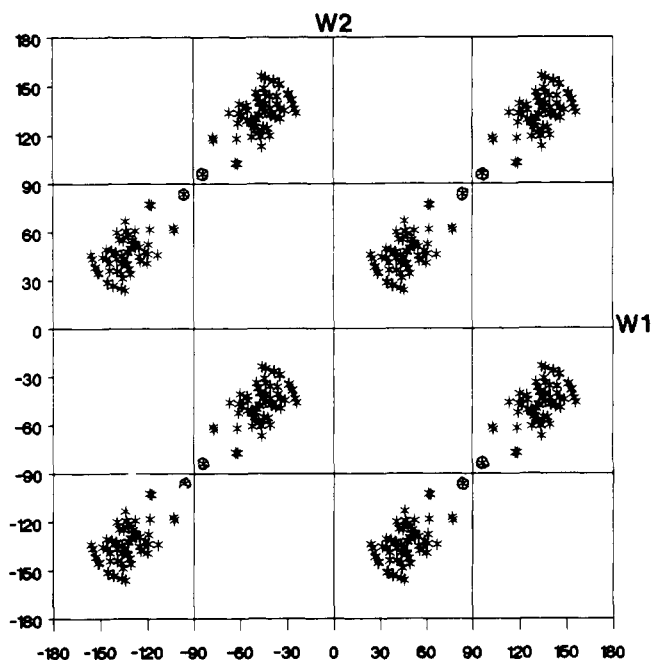


Figure 11. Conformational map ( $w_1$  vs  $w_2$ ) for  $\text{Ar}_2\text{C}=\text{CR}_2$ : (☆) compound **10**, Table S31.

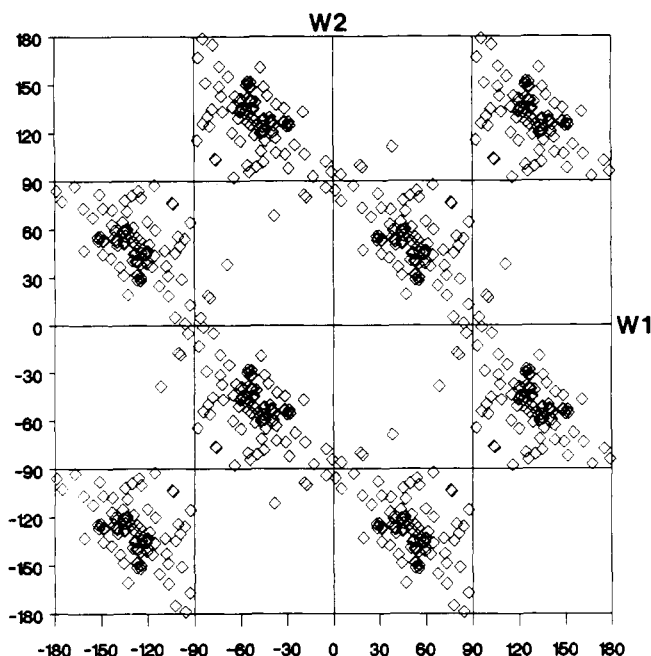


Figure 12. Conformational map ( $w_1$  vs  $w_2$ ) for  $\text{Ar}_2\text{C}=\text{CR}^1\text{R}^2$ ,  $\text{Ar} \neq \text{Mes}$ .

the symmetrical (i.e.,  $R^1 = R^2$ ) systems, especially where  $R = H$ . This is clearly demonstrated in Figure 11, which gives the map for subgroup a. We conclude that a two-ring flip is also a likely possibility, especially when the R's are bulky.

If the density of the points along the two pathways can serve as a rough guide to the importance of the one-ring and the two-ring flip routes, the energy difference, at least for the 1,1-diphenyl moiety, between the two routes is not excessively large. This is consistent with the results of the calculations for **8**.

(d) Comparison of the maps of nonsubstituted or para-substituted 1,1-diphenyl and 1,1-dimesityl moieties is shown in Figure 12 and Figure S6. The points in Figure S6 mostly represent the presently determined  $\text{Mes}_2\text{C}=\text{C}(\text{OH})\text{R}$  systems, and those in Figure 12 represent  $\text{Ar}_2\text{C}=\text{CHR}$  systems with less hindered aryl groups. Although the number of dimesityl derivatives is limited, the comparison shows that these points extend slightly away from

(35) Biali, S. E.; Gozin, M.; Rappoport, Z. *J. Phys. Org. Chem.* **1989**, *2*, 271.

(36) Berkovitch-Yellin, Z.; Leiserowitz, L. *Acta Crystallogr., Sect. B.* **1977**, *B33*, 3567.

the (40°, 40°) region in the (90°, 90°) direction, whereas the points out of the (40°, 40°) minimum in Figure 12 extend in the (0°, 90°) and (90°, 0°) directions. The conclusion for molecules **1a-e** and **4** investigated in the present paper is that both the one- and the two-ring flips are feasible, in line with the experimental observation.<sup>5a,b</sup>

(e) It is interesting to see the structures that set the trends along the pathways. There are 11 structures with one torsional angle ( $\leq 25^\circ$ ), and except for two of them,  $\Delta\phi = \phi_1 - \phi_2 > 25^\circ$ . Of these, seven structures with  $\Delta\phi > 55^\circ$  are organometallic derivatives (entries 47–51, 52b, Table S31; **10–15**, Chart I). Other structures in which  $\Delta\phi > 25$  but  $\phi_1, \phi_2 > 25^\circ$  include an organoplatinum derivative (entry 34, Table S31; **16**), five structures with a  $\text{Ph}_2\text{C}=\text{C}$  moiety exocyclic to a ring, and five  $\text{Ph}_2\text{C}=\text{CR}^1\text{R}^2$  structures where  $\text{R}^1$  and  $\text{R}^2$  differ much in their bulk.

The large  $\Delta\phi$  values encountered with organometallic derivatives raise the question whether, due to the interaction with the metal, the  $\text{Ph}_2\text{C}=\text{C}$  moiety still remains as intact as possible. This problem was probed in two ways: First, the C=C bond lengths when  $\Delta\phi > 55^\circ$  are 1.328–1.357 Å for four structures, which is within the experimental error of the average C=C bond length. Only for an osmium complex (entry 51a, Table S31) the C=C bond lengths in the two crystal forms were out of this region, but in opposite directions, they were 1.320 and 1.362 Å, respectively. Second, pyramidalization of the double bond should be detected by a large deviation of the sum of the three bond angles in the diphenyl-substituted carbon from 360°. However, these differences for the systems in question are negligible in all cases.

(f) It is interesting that the number of “symmetrical” cims with crystallographic  $C_2$  symmetry (i.e.,  $\phi_1 = \phi_2$ ) is only six (five compounds). The most interesting of these is 1,1-bis(2-hydroxy-3-nitro-5-chlorophenyl)-2,2-dichloroethylene (entry 10, Table S31), where  $\phi = 83.7^\circ$ , apparently due to steric effects of the ortho-substituents. Also interesting is the 1,1-bis(*p*-ethoxyphenyl)ethylene (entry 3, Table S31), where the  $\phi$  value of  $36.2^\circ$  is somewhat lower than the calculated angle for 1,1-diphenyl-ethylene. If the comparison of a calculated and an experimental value is valid, the difference may reflect the higher stabilizing resonant Ar—C=C interactions for Ar = *p*-ethoxyphenyl compared with Ar = Ph.

**Structural Correlations in 1,1-Diarylvinyl Propellers.** (a) **Small Subgroups.** (i) Data are available for  $\text{Ar}_2\text{C}=\text{CR}_2$  substituted in the para position by substituents of different electronic demands (R = H, Ar = *p*-Tol, *p*-O<sub>2</sub>NC<sub>6</sub>H<sub>4</sub>, *p*-EtOC<sub>6</sub>H<sub>4</sub>; R = Cl, Ar = *p*-MeOC<sub>6</sub>H<sub>4</sub>, *p*-ClC<sub>6</sub>H<sub>4</sub>) (entries 1–3, 8, and 9, Table S31). Interestingly, when R = H moderate differences are observed between the bond angles or  $\phi_1$  of the different compounds whereas  $\phi_2$  changes by 12.4°. This is of interest in relation to the extent of “perturbation” of the diarylvinyl moiety by the para substituent, but there are not sufficient data to detect a trend, if present. (ii) In compounds (*p*-AcOC<sub>6</sub>H<sub>4</sub>)<sub>2</sub>C=C(CH<sub>2</sub>)<sub>n</sub>-c (entries 4–7, Table S31) one of the vinylic carbons belongs to a cycloalkane ring. Although intuition suggests that the smaller the cycloalkane ring, the larger the C=C—C(sp<sup>3</sup>) angle, and the smaller the torsion angles, no clear trend is observed for  $n = 3$ –5, 7, except that  $\phi$

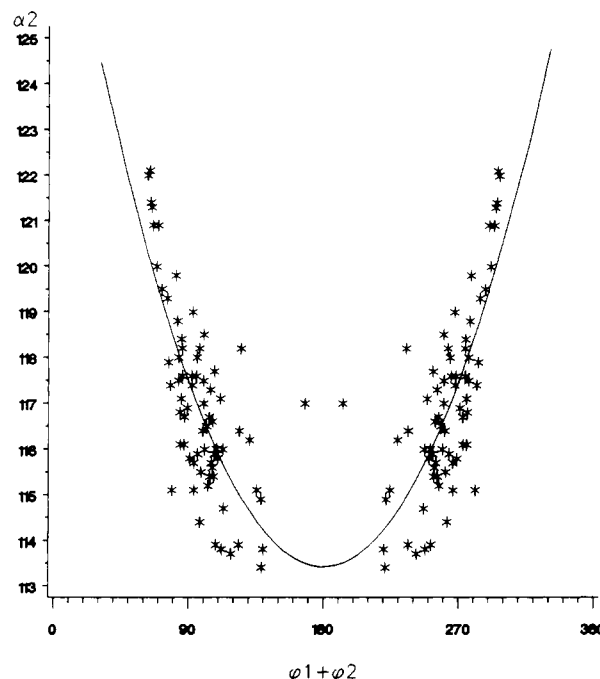
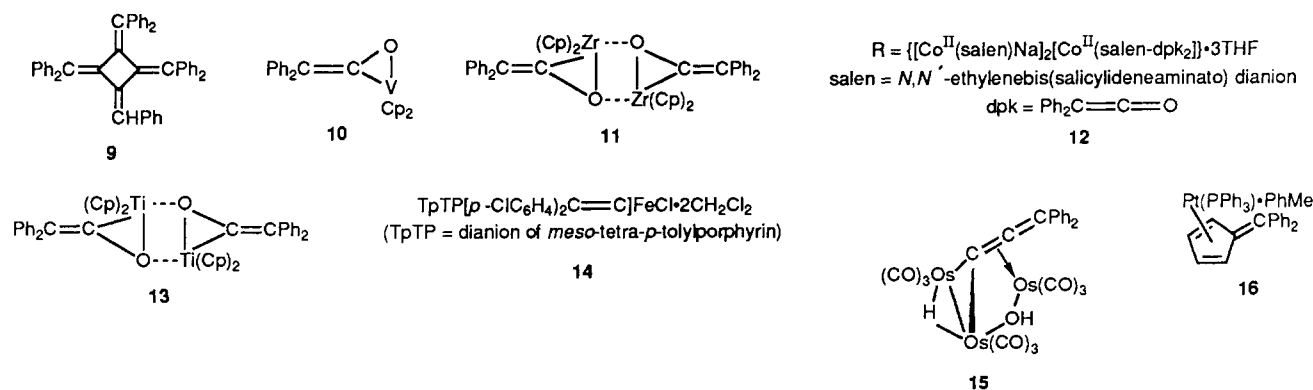


Figure 13. Plot of  $\alpha_2$  vs the sum of the torsional angles ( $\phi_1 + \phi_2$ ) for 1,1-diarylvinyl derivatives.

increases approximately linearly with  $n$  from  $0^\circ$  ( $n = 3$ ) to  $15 \pm 1^\circ$  ( $n = 7$ ).

(b) **Complete Set. Other Correlations of Bond Angles, Torsional Angles, and Bond Lengths.** Clear trends exist between several sets of parameters of 1,1-diarylethylenes. A plot of the bond angle vs the torsional angle of the aryl ring on the opposite side, i.e.  $\alpha_1$  vs  $\phi_1$  together with  $\alpha_3$  vs  $\phi_2$ , shows a monotonic increase with an appreciable scatter of the points:  $\alpha = 117.52 + 0.083\phi$  (Sd = 0.015) (Figure S7). A similar trend is found in the plot of a bond angle vs the contiguous torsional angle, i.e.  $\alpha_1$  vs  $\phi_2$  together with  $\alpha_3$  vs  $\phi_1$ :  $\alpha = 118.19 + 0.068\phi$  (Sd = 0.016) (Figure S8). The problem with these plots, however, is that an arbitrary decision is made in choosing which angle is  $\phi_1$  and which is  $\phi_2$ . We overcame this problem by plotting the bond angle  $\alpha_2$  vs the sum of the torsional angles  $\phi_1 + \phi_2$ . Due to the periodicity of the torsional angles, each point was introduced twice, at  $\phi_1 + \phi_2$  and at  $360 - (\phi_1 + \phi_2)$ . Figure 13 shows that there is a monotonous decrease (with scatter) of  $\alpha_2$  with the increase of  $\phi_1 + \phi_2$ , and an analytical form that approximately fits the observed curve is a parabola. The larger deviation at large  $\phi_1 + \phi_2$  value may indicate that the increase at this region is steeper than that shown in Figure 13. A clear deviation is (2-HO-3-O<sub>2</sub>N-5-ClC<sub>6</sub>H<sub>2</sub>)<sub>2</sub>C=C=CCl<sub>2</sub> (compound **10**, Table S31), for which  $\phi_1 + \phi_2 = 167^\circ$ , but this compound also deviates from other correlations. This correlation is an outcome of the geometry of the systems. As shown by the MM calculations in the idealized transition state

Chart I



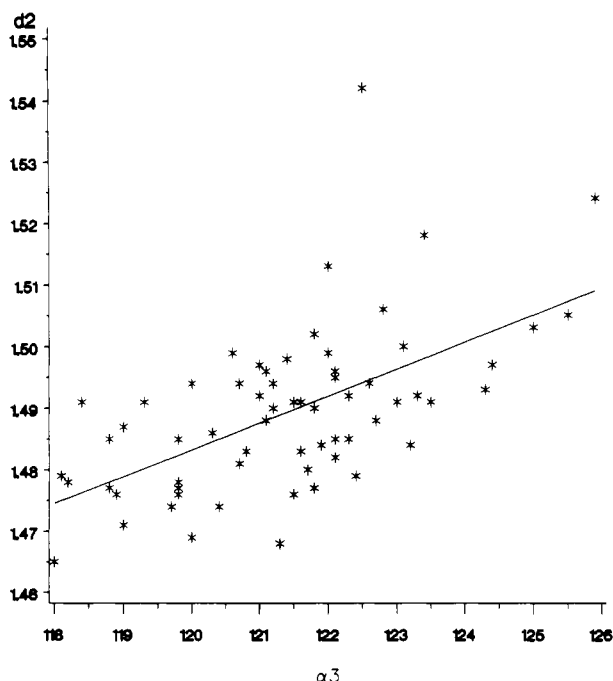


Figure 14. Plot of the C—Ar bond length  $d$  vs the corresponding C=C—Ar bond angle  $\alpha$ .

of the two-rings flip ( $\phi_1 + \phi_2 = 180^\circ$ ),  $\alpha_2$  is smaller than its value in the ground-state conformation (Table IV).

A similar type of correlation exists between the C—Ar bond length  $d_2$  and the ArC=C ( $\alpha_1$  or  $\alpha_3$ ) angle associated with the same aryl ring. Both C—Ar bonds and their  $\alpha$  values can be included in the same correlation. A plot for the symmetrical (i.e.,  $R^1 = R^2$ ) 1,1-diarylethenes is shown in Figure 14. Disregarding an abnormally long C—Ar bond length of 1.54 Å, the trend is clear:  $d_2$  increases with  $\alpha$ ,  $d = 0.960 + 0.04\alpha$  ( $S_d = 0.007$ ).

The correlation results from a response of the two parameters in the same direction to the presence of bulky substituents on C(2). The steric interactions caused by the bulkier substituents cis to the  $\beta$ -aryl rings are relieved not only by rotation of the rings but by opening the bond angles involving these rings and by elongating the C—Ar bond.

**Conclusions.** The stable enols 1-R-2,2-dimesitylethenols ( $R = H, Me, Et, i\text{-}Pr, t\text{-}Bu$ ) exist in a propeller conformation in the crystal. The structural parameters of the enols are related to the steric bulk of the R substituent. Analysis of crystal data of molecules containing the  $Ar_2C=C$  fragment together with molecular mechanics calculations indicate that both the one- and two-ring flip mechanisms are feasible pathways for the helicity reversal process, whereas the zero-ring flip is energetically inaccessible.

## Experimental Section

Intensity was measured with a Philips PW 1100 four-circle diffractometer with graphite-monochromated Mo K $\alpha$  radiation (0.71069 Å).

The crystal structures were solved by MULTAN 77<sup>37</sup> or by SHELX<sup>38</sup> and refined by the latter. The refinement procedure was carried out in the following ways: For **1a** each of the four independent molecules was refined in a separate block with anisotropic temperature factors for the non-hydrogen atoms and isotropic for the H atoms. The H atoms in each methyl group were assigned with equal temperature factors. All the hydrogens except the hydroxyl one were tied in a fixed geometry with the C atoms during the refinement. In **1b** the enol and the solvent molecule were refined in separate blocks. In **1c** all atoms were refined in one block, while in **1d**, **1e**, and **4** the heavy atoms and the hydrogen atoms were refined in separate blocks.

**2,2-Dimesitylethenol (1a):**  $C_{20}H_{24}O$ ; monoclinic;  $a = 21.182$  (11),  $b = 14.308$  (7),  $c = 22.938$  (12) Å;  $\beta = 97.02$  (3) $^\circ$ ; space group  $P2_1/c$ ;  $Z = 16$ ;  $R = 0.103$ ,  $R_w = 0.090$  for 5008 reflections [ $F_o > 1.5\sigma F_o$ ;  $w = 1.5096/(\sigma^2 F + 0.0005 F^2)$ ].

**1,1-Dimesitylpropen-2-ol (1b):**  $C_{21}H_{26}O \cdot C_2H_5OH$ ; triclinic;  $a = 12.314$  (6),  $b = 11.079$  (6),  $c = 8.347$  (4) Å;  $\alpha = 109.08$  (3),  $\beta = 92.34$  (3),  $\gamma = 101.39$  (3) $^\circ$ ; space group  $P\bar{1}$ ;  $Z = 2$ ;  $R = 0.095$ ,  $R_w = 0.099$  for 2165 reflections [ $F_o > 1.5\sigma F_o$ ;  $w = 3.9512/(\sigma^2 F + 0.0003 F^2)$ ].

**1,1-Dimesityl-1-buten-2-ol (1c):**  $C_{22}H_{28}O$ ; monoclinic;  $a = 19.593$  (10),  $b = 11.834$  (6),  $c = 17.749$  (9) Å;  $\beta = 113.99$  (3) $^\circ$ ; space group  $P2_1/c$ ;  $Z = 8$ ;  $R = 0.087$ ,  $R_w = 0.082$  for 3244 reflections [ $F_o > 1.5\sigma F_o$ ;  $w = 1.6029/(\sigma^2 F + 0.0010 F^2)$ ].

**1,1-Dimesityl-3-methyl-1-buten-2-ol (1d):**  $C_{23}H_{30}O$ ; monoclinic;  $a = 14.381$  (7),  $b = 15.494$  (8),  $c = 8.720$  (4) Å;  $\beta = 92.18$  (2) $^\circ$ ; space group  $P2_1/c$ ;  $Z = 4$ ;  $R = 0.094$ ,  $R_w = 0.075$  for 1734 reflections [ $F_o > 1.5\sigma F_o$ ;  $w = 1.5932/(\sigma^2 F + 0.0001 F^2)$ ].

**1,1-Dimesityl-3,3-dimethyl-1-buten-2-ol (1e):**  $C_{24}H_{32}O$ ; triclinic;  $a = 11.757$  (6),  $b = 11.449$  (5),  $c = 8.329$  (4) Å;  $\alpha = 108.62$  (3),  $\beta = 107.11$  (3),  $\gamma = 89.55$  (3) $^\circ$ ; space group  $P\bar{1}$ ;  $Z = 2$ ;  $R = 0.073$ ,  $R_w = 0.080$  for 2424 reflections [ $F_o > 1.5\sigma F_o$ ;  $w = 1.6293/(\sigma^2 F + 0.024 F^2)$ ].

**1,1-Dimesitylethylene (4):**  $C_{20}H_{24}$ ; monoclinic;  $a = 8.479$  (4),  $b = 7.866$  (4),  $c = 24.202$  (12) Å;  $\beta = 94.53$  (2) $^\circ$ ; space group  $P2_1/c$ ;  $Z = 4$ ;  $R = 0.103$ ,  $R_w = 0.080$  for 1346 reflections [ $F_o > 2.0\sigma F_o$ ;  $w = 1.6168/(\sigma^2 F + 0.0002 F^2)$ ].

Statistical analysis system (SAS/GRAPH, 1985 version) was used for plotting the conformational maps and for the correlations.

**Acknowledgment.** We are grateful to the United States–Israel Binational Science Foundation (BSF), Jerusalem, Israel, The Bat-Sheva de Rothschild Fund, and the Fund for the Promotion of Research at the Technion who supported the work. We also thank I. Agmon for helping in the determination of the crystal structure of **1d**.

**Supplementary Material Available:** Tables S1–S30 of bond lengths, bond angles, positional parameters, and thermal parameters for **1a–1e** and **4**, and Tables S31 and S32 containing crystallographic data from the literature for  $Ar_2C=CR^1R^2$  and  $Ar^1Ar^2C=C(R)Ar^3$ , and Figures S1–S8 showing stereoscopic views of the packing arrangements of **1a** and **1b**, histograms of frequency of appearance vs C(1)=C(2) bond lengths, conformational maps, and  $\alpha$  vs  $\phi$  plots (56 pages); listings of observed and calculated structure factors (93 pages). Ordering information is given on any current masthead page.

(37) Main, P.; Fiske, S. J.; Hull, S. E.; Lessinger, L.; Germain, G.; Declercq, S.-P.; Woolfson, M. M., MULTAN 80. A system of computer programs for the automatic solution of crystal structures from X-ray diffraction data, University of York, England, and Louvain, Belgium.

(38) Sheldrick, G. M. SHELX-76, Program for crystal structure determination, University of Cambridge, 1976.